

# Crystal structure and luminescence of a europium 3-methoxybenzoate complex with 2,2'-bipyridine

Xia Li<sup>a,b</sup>, Zuqiang Bian<sup>a</sup>, Linpei Jin<sup>a,\*</sup>, Shaozhe Lu<sup>c</sup>, Shihua Huang<sup>c</sup>

<sup>a</sup>Department of Chemistry, Beijing Normal University, Beijing 100875, People's Republic of China

<sup>b</sup>Department of Chemistry, Capital Normal University, Beijing 100037, People's Republic of China

<sup>c</sup>Laboratory of Excited State Processes, Chinese Academy of Sciences, Changchun 130021, People's Republic of China

Received 28 June 1999; received in revised form 16 August 1999; accepted 16 August 1999

## Abstract

The structure of the dimer  $[\text{Eu}(m\text{-MOBA})_3 \cdot 2,2'\text{-bipy}]_2$  (*m*-MOBA: *m*-methoxybenzoate, 2,2'-bipy: 2,2'-bipyridine) was determined by single crystal X-ray diffraction. Each europium atom is coordinated with two oxygen atoms of the chelated carboxyl group, four oxygen atoms of the bidentate bridging carboxylate groups and two nitrogen atoms from a 2,2'-bipyridine molecule forming a dimeric structure with coordination number 8. The luminescence behaviour of the  $\text{Eu}^{3+}$  ion in  $[\text{Eu}(m\text{-MOBA})_3 \cdot 2,2'\text{-bipy}]_2$  was observed at 77 K. The emission spectra of  ${}^5\text{D}_1 \rightarrow {}^7\text{F}_J$  ( $J = 1-3$ ) and  ${}^5\text{D}_0 \rightarrow {}^7\text{F}_J$  ( $J = 0-4$ ) transitions were measured. The complex displays intense luminescence and the  $\text{Eu}^{3+}$  ions in the dimer occur in slightly different chemical environments. © 2000 Elsevier Science B.V. All rights reserved.

**Keywords:** X-ray crystallography; Europium complex; Luminescence property

## 1. Introduction

A number of ternary lanthanide complexes of benzoic acid and its derivatives with 2,2'-bipyridine (2,2'-bipy) have been reported [1–6]. The characteristics of these complexes are the dimeric structures through the bridging linkage of the carboxyl groups. The bonding modes differ from similar lanthanide complexes with 4,4'-bipyridine in which water molecules are involved in coordination and the infinite polymeric chain is composed of the bridging carboxyl groups [7]. Among these ternary complexes europium complexes display intense fluorescence. Observations of the high-resolution spectra of the europium complexes show that the  $\text{Eu}^{3+}$  ion sites have low

symmetry, which is in agreement with the results of X-ray analysis. As a part of a series of our study on ternary europium complexes this paper reports the structure of the europium *m*-methoxybenzoate (*m*-MOBA) complex with 2,2'-bipyridine and the emission spectra of the complex.

## 2. Experimental

### 2.1. Synthesis of $\text{Eu}(m\text{-MOBA})_3 \cdot 2,2'\text{-bipy}$

3 mmol *m*-HMOBA and 1 mmol 2,2'-bipy were dissolved in 25 ml 95%  $\text{C}_2\text{H}_5\text{OH}$ . The pH of the solution was adjusted to  $\sim 6.5$  with 1 mol  $\text{dm}^{-3}$  NaOH solution. To the resulting clear solution was added 1 mmol  $\text{EuCl}_3$  solution (dissolved in 5 ml  $\text{H}_2\text{O}$ ). The reaction was stirred for 5 h at 60–70°C. A white

\* Corresponding author. Fax: +86-10-6220-0567.

E-mail address: lpjin@bnu.edu.cn (L. Jin).

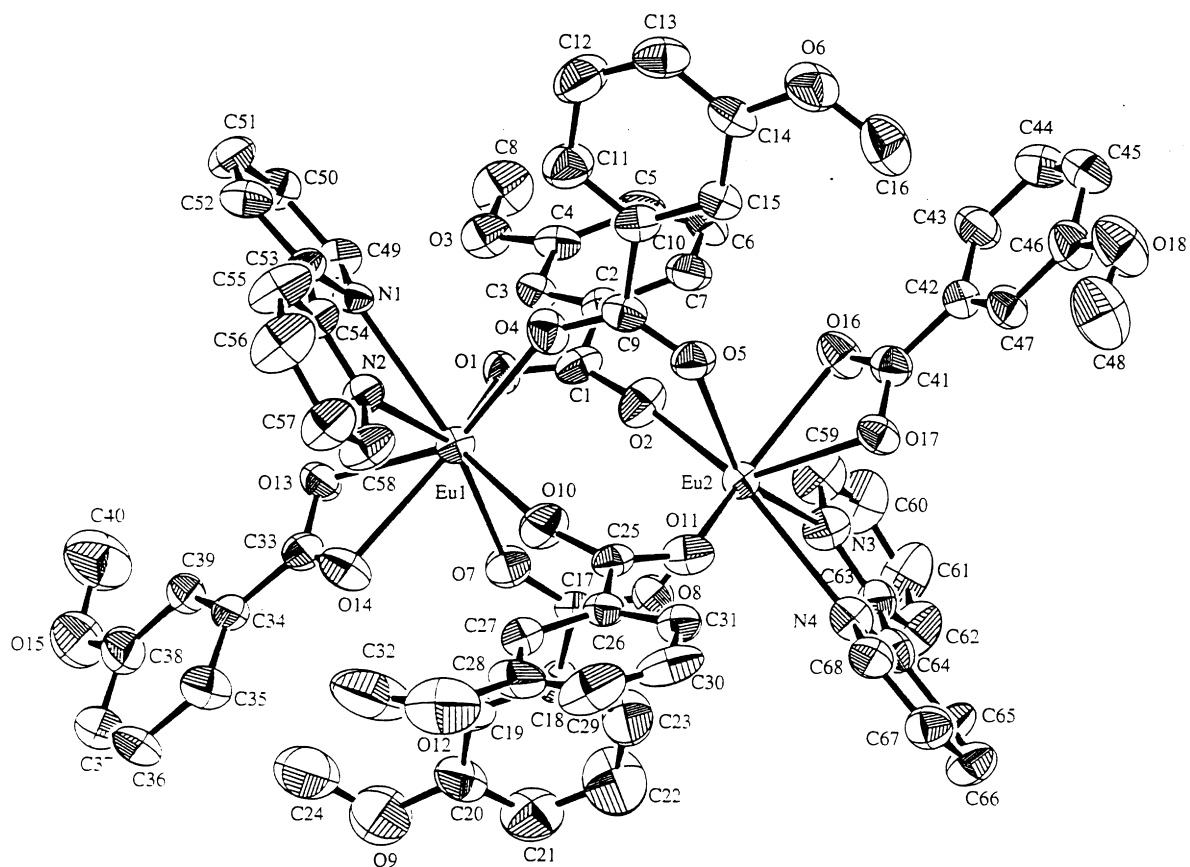
Fig. 1. Molecular structure of  $\text{Eu}(m\text{-MOBA})_3 \cdot 2,2'\text{-bipy}$ .

Table 1

Crystal data for  $\text{Eu}(m\text{-MOBA})_3 \cdot 2,2'\text{-bipy}$ 

Formula weight	1523.14
Temperature	293 K
Radiation (Mo $K_\alpha$ )	0.71069 Å
Crystal system	Monoclinic
Space group	Pc
Unit cell dimensions	$a = 10.546(2)$ Å $b = 16.039(6)$ Å $c = 18.944(3)$ Å $\beta = 101.95(1)^\circ$
Volume	$3134(1)$ Å <sup>3</sup>
Z	2
Density (calculated)	$1.614$ g cm <sup>-3</sup>
Absorption coefficient	$20.55$ cm <sup>-1</sup>
$F(000)$	1528.00
Crystal size	$0.20 \times 0.20 \times 0.30$ mm <sup>3</sup>
$2\theta_{\text{max}}$	$50.0^\circ$
Index ranges	$0 \leq h \leq 11, 0 \leq k \leq 19,$ $-22 \leq l \leq 22$
Reflections collected	5024
Independent reflections	4696 ( $R_{\text{int}} = 0.064$ )
Data/restraints/parameters	4176/0/828
Goodness-of-fit on $F^2$	1.38
Final R indices [ $I(2\sigma(I))$ ]	$R_1 = 0.023, \omega R_2 = 0.031$
Largest diff. peak and hole	$0.44$ and $-0.34$ eÅ <sup>-3</sup>

precipitate was formed. Crystals of  $\text{Eu}(m\text{-MOBA})_3 \cdot 2,2'\text{-bipy}$  suitable for X-ray analysis were obtained from the mother liquor after 2 weeks.

## 2.2. Crystal structure determination

X-ray data were collected for the title complex on a Rigaku APCR diffractometer at 293 K using graphite monochromated Mo  $K_\alpha$  radiation. An empirical absorption correction using the program DIFABS was applied [8]. The structure was solved by heavy-atom Patterson methods. Non-hydrogen atoms were refined anisotropically while hydrogen atoms were included but not refined. All calculations were performed using the software package [9]. Crystal data and experimental details are listed in Table 1.

Table 2  
Non-hydrogen atomic coordinates and thermal parameters  $B(\text{eq})$

Atom	$x$	$y$	$z$	$B(\text{eq})$
Eu(1)	0.0060	0.24393(2)	0.0030	3.05(1)
Eu(2)	0.26959(4)	0.24264(2)	-0.14355(2)	3.11(1)
O(1)	-0.1159(6)	0.2650(4)	-0.1154(3)	4.1(1)
O(2)	0.0528(7)	0.2636(4)	-0.1669(4)	4.7(2)
O(3)	-0.4907(5)	0.2713(4)	-0.3242(3)	4.8(1)
O(4)	0.0906(6)	0.3728(4)	-0.0234(3)	4.6(1)
O(5)	0.2535(6)	0.3720(3)	-0.0822(3)	4.3(1)
O(6)	0.3761(7)	0.6794(4)	-0.0833(4)	6.4(2)
O(7)	0.0379(7)	0.1169(4)	-0.0552(4)	4.8(2)
O(8)	0.1875(6)	0.1103(3)	-0.1221(4)	4.5(1)
O(9)	-0.142(1)	-0.1817(5)	-0.0747(6)	10.6(3)
O(10)	0.2333(7)	0.2232(5)	0.0421(4)	5.7(2)
O(11)	0.3851(6)	0.2188(4)	-0.0239(3)	4.4(1)
O(12)	0.502(1)	0.1583(6)	0.2986(5)	10.8(3)
O(13)	-0.1762(7)	0.1674(4)	0.0209(4)	4.3(1)
O(14)	0.0038(7)	0.1366(4)	0.0980(4)	5.0(2)
O(15)	-0.492(1)	-0.0643(4)	0.0473(6)	9.2(3)
O(16)	0.2556(7)	0.3465(4)	-0.2401(3)	4.7(2)
O(17)	0.4461(6)	0.3262(4)	-0.1703(3)	3.9(1)
O(18)	0.7152(7)	0.5734(5)	-0.2204(5)	7.9(2)
N(1)	-0.1774(7)	0.3513(5)	0.0167(4)	3.2(2)
N(2)	0.0290(7)	0.3241(5)	0.1247(4)	3.8(2)
N(3)	0.2414(7)	0.1641(5)	-0.2650(4)	4.5(2)
N(4)	0.4574(8)	0.1437(5)	-0.1650(4)	3.5(2)
C(1)	-0.0669(8)	0.2729(5)	-0.1696(4)	3.9(2)
C(2)	-0.1533(7)	0.2971(4)	-0.2395(4)	3.4(2)
C(3)	-0.2826(7)	0.2791(5)	-0.2511(4)	3.5(2)
C(4)	-0.3648(8)	0.2956(4)	-0.3189(4)	3.9(2)
C(5)	-0.313(1)	0.3304(6)	-0.3720(4)	5.2(2)
C(6)	-0.183(1)	0.3513(6)	-0.3593(5)	5.7(3)
C(7)	-0.1002(8)	0.3342(5)	-0.2939(5)	4.5(2)
C(8)	-0.577(1)	0.2853(7)	-0.3912(5)	6.5(3)
C(9)	0.1744(8)	0.4074(4)	-0.0505(4)	3.9(2)
C(10)	0.1833(7)	0.5015(4)	-0.0426(4)	3.7(2)
C(11)	0.095(1)	0.5449(5)	-0.0142(5)	5.6(2)
C(12)	0.099(1)	0.6325(6)	-0.0118(6)	6.9(3)
C(13)	0.193(1)	0.6740(5)	-0.0347(5)	5.5(2)
C(14)	0.2853(8)	0.6303(4)	-0.0628(4)	4.1(2)
C(15)	0.2799(7)	0.5440(4)	-0.0675(4)	3.5(2)
C(16)	0.479(1)	0.6403(7)	-0.1068(7)	7.7(3)
C(17)	0.0966(8)	0.0809(4)	-0.0969(4)	3.4(2)
C(18)	0.0556(7)	-0.0071(5)	-0.1169(4)	3.8(2)
C(19)	-0.0272(8)	-0.0509(5)	-0.0823(4)	4.4(2)
C(20)	-0.0609(8)	-0.1320(6)	-0.1050(6)	6.3(3)
C(21)	-0.014(1)	-0.1683(6)	-0.1602(7)	7.6(3)
C(22)	0.062(2)	-0.1240(7)	-0.1954(7)	9.5(4)
C(23)	0.100(1)	-0.0453(6)	-0.1744(6)	7.3(3)
C(24)	-0.211(2)	-0.1470(8)	-0.0336(8)	9.2(4)
C(25)	0.3482(7)	0.2150(5)	0.0352(4)	3.5(2)
C(26)	0.4496(7)	0.2036(4)	0.1024(4)	3.5(2)
C(27)	0.416(1)	0.1806(5)	0.1657(5)	5.4(2)
C(28)	0.516(2)	0.1746(6)	0.2294(5)	7.8(3)

Table 2 (continued)

Atom	$x$	$y$	$z$	$B(\text{eq})$
C(29)	0.640(1)	0.1918(7)	0.2262(6)	7.6(3)
C(30)	0.673(1)	0.2127(6)	0.1652(6)	5.9(2)
C(31)	0.5783(8)	0.2194(5)	0.1021(4)	3.9(2)
C(32)	0.384(1)	0.1407(8)	0.301(1)	11.7(5)
C(33)	-0.114(1)	0.1219(6)	0.0694(5)	4.4(3)
C(34)	-0.182(1)	0.0471(5)	0.0934(5)	4.5(2)
C(35)	-0.116(1)	-0.0021(6)	0.1496(6)	6.4(3)
C(36)	-0.184(1)	-0.0738(7)	0.1682(7)	8.5(4)
C(37)	-0.305(2)	-0.0896(7)	0.1338(9)	8.9(4)
C(38)	-0.368(1)	-0.0393(6)	0.0782(6)	6.5(3)
C(39)	-0.309(1)	0.0300(5)	0.0579(5)	4.5(2)
C(40)	-0.562(1)	-0.0110(8)	-0.0064(8)	9.2(4)
C(41)	0.373(1)	0.3675(5)	-0.2196(4)	3.8(2)
C(42)	0.4237(8)	0.4426(5)	-0.2518(5)	4.0(2)
C(43)	0.3475(9)	0.4856(6)	-0.3073(5)	5.2(2)
C(44)	0.396(1)	0.5544(6)	-0.3339(5)	6.0(3)
C(45)	0.515(1)	0.5837(6)	-0.3038(6)	6.3(3)
C(46)	0.596(1)	0.5400(5)	-0.2460(5)	5.5(2)
C(47)	0.548(1)	0.4701(6)	-0.2218(5)	4.3(2)
C(48)	0.791(1)	0.5360(9)	-0.1625(7)	8.8(4)
C(49)	-0.2877(7)	0.3554(4)	-0.0336(4)	3.8(2)
C(50)	-0.3933(7)	0.4035(5)	-0.0253(4)	4.0(2)
C(51)	-0.3830(9)	0.4504(5)	0.0355(5)	4.9(2)
C(52)	-0.269(1)	0.4447(6)	0.0881(5)	4.5(2)
C(53)	-0.1722(8)	0.3967(5)	0.0767(4)	3.3(2)
C(54)	-0.0536(7)	0.3840(4)	0.1340(4)	3.5(2)
C(55)	-0.028(1)	0.4328(6)	0.1963(5)	5.9(2)
C(56)	0.078(1)	0.4141(7)	0.2523(5)	6.7(3)
C(57)	0.157(1)	0.3493(6)	0.2421(5)	5.8(2)
C(58)	0.1296(8)	0.3070(6)	0.1776(4)	5.1(2)
C(59)	0.1361(8)	0.1798(6)	-0.3171(5)	5.6(2)
C(60)	0.109(1)	0.1361(7)	-0.3811(5)	6.6(3)
C(61)	0.188(1)	0.0750(8)	-0.3936(6)	7.3(3)
C(62)	0.297(1)	0.0593(6)	-0.3421(5)	6.5(3)
C(63)	0.3215(8)	0.1056(5)	-0.2782(4)	4.1(2)
C(64)	0.445(1)	0.0966(6)	-0.2246(4)	3.9(2)
C(65)	0.546(1)	0.0439(6)	-0.2359(5)	4.8(2)
C(66)	0.661(1)	0.0415(6)	-0.1869(5)	5.3(2)
C(67)	0.6720(8)	0.0932(5)	-0.1269(5)	4.7(2)
C(68)	0.5712(8)	0.1411(5)	-0.1174(4)	4.0(2)

Table 3  
Selected bond lengths ( $\text{\AA}$ )

Eu(1)	O(1)	2.366(6)	Eu(2)	O(2)	2.262(7)
Eu(1)	O(4)	2.346(6)	Eu(2)	O(5)	2.401(5)
Eu(1)	O(7)	2.374(6)	Eu(2)	O(8)	2.359(6)
Eu(1)	O(10)	2.381(7)	Eu(2)	O(11)	2.372(6)
Eu(1)	O(13)	2.364(7)	Eu(2)	O(16)	2.455(6)
Eu(1)	O(14)	2.495(6)	Eu(2)	O(17)	2.431(6)
Eu(1)	N(1)	2.642(8)	Eu(2)	N(3)	2.586(8)
Eu(1)	N(2)	2.607(7)	Eu(2)	N(4)	2.634(8)

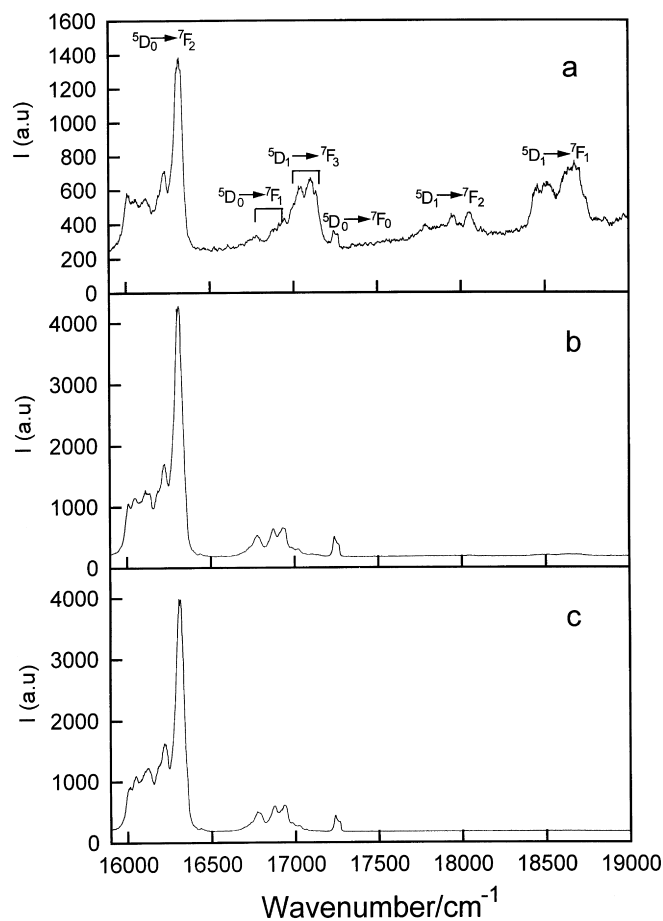


Fig. 2. Time resolved spectra of  $\text{Eu}(m\text{-MOBA})_3 \cdot 2,2'\text{-bipy}$   $\lambda_{\text{exc}} = 337.1 \text{ nm}$ , 77 K: (a) delay time: 2  $\mu\text{s}$ ; (b) delay time: 20  $\mu\text{s}$ ; (c) delay time: 30  $\mu\text{s}$ .

### 2.3. Excitation and emission spectral measurement

The emission spectra were measured with an HRG.9-5-90  $\text{N}_2$  laser at 77 K using a Spex 1403 double grating monochromator. The high resolution spectrum was obtained at 77 K using a PLT-2000 dye laser (rhodamine 6G) pumped by  $\text{N}_2$  laser.

## 3. Results and discussion

The molecular structure of  $[\text{Eu}(m\text{-MOBA})_3 \cdot 2,2'\text{-bipy}]_2$  is shown in Fig. 1. The atomic coordinates and thermal parameters are listed in Table 2 while selected bond lengths and bond angles are tabulated

in Tables 3 and 4, respectively. Fig. 1 shows that the coordinated atoms around each europium atom consist of two oxygen atoms from the bidentate chelated carboxyl group, four oxygen atoms from the four carboxylato-*o,o'*-bridged groups and two nitrogen atoms of a 2,2'-bipyridine molecule. Unlike  $\{[\text{Eu}(m\text{-MOBA})_3 \cdot \text{H}_2\text{O}] \cdot 1/2 \text{ 4,4}'\text{-bipy}\}_\infty$  [7],  $[\text{Eu}(m\text{-MOBA})_3 \cdot 2,2'\text{-bipy}]_2$  is a centrosymmetric tetrakis-(carboxylato-*o,o'*)-bridged dimer, in which the carboxylato groups act as the bidentate chelated and bidentate bridging coordination modes which are common in the dimeric lanthanide carboxylate complexes. The average  $\text{Eu}(1)\text{-O}$  distance (2.388 Å) is comparable to the average  $\text{Eu}(2)\text{-O}$  distance (2.382 Å) found in the dimer. However, the average

Table 4  
Selected bond angles (°)

O(1)	Eu(1)	O(4)	80.1(2)	O(2)	Eu(2)	O(5)	78.2(2)
O(1)	Eu(1)	O(7)	77.5(2)	O(2)	Eu(2)	O(8)	77.0(2)
O(1)	Eu(1)	O(10)	129.0(2)	O(2)	Eu(2)	O(11)	120.6(2)
O(1)	Eu(1)	O(13)	85.0(2)	O(2)	Eu(2)	O(16)	81.4(2)
O(1)	Eu(1)	O(14)	134.2(2)	O(2)	Eu(2)	O(17)	131.6(2)
O(1)	Eu(1)	N(1)	74.6(2)	O(2)	Eu(2)	N(3)	88.5(2)
O(1)	Eu(1)	N(2)	134.5(2)	O(2)	Eu(2)	N(4)	145.2(2)
O(4)	Eu(1)	O(7)	124.2(2)	O(5)	Eu(2)	O(8)	129.0(2)
O(4)	Eu(1)	O(10)	77.7(2)	O(5)	Eu(2)	O(11)	75.5(2)
O(4)	Eu(1)	O(13)	147.6(2)	O(5)	Eu(2)	O(16)	77.0(2)
O(4)	Eu(1)	O(14)	145.3(2)	O(5)	Eu(2)	O(17)	76.0(2)
O(4)	Eu(1)	N(1)	76.4(2)	O(5)	Eu(2)	N(3)	147.7(2)
O(4)	Eu(1)	N(2)	77.5(2)	O(5)	Eu(2)	N(4)	136.5(2)
O(7)	Eu(1)	O(10)	78.1(3)	O(8)	Eu(2)	O(11)	79.9(2)
O(7)	Eu(1)	O(13)	79.5(2)	O(8)	Eu(2)	O(16)	140.4(2)
O(7)	Eu(1)	O(14)	76.4(2)	O(8)	Eu(2)	O(17)	148.9(2)
O(7)	Eu(1)	N(1)	141.5(2)	O(8)	Eu(2)	N(3)	74.7(2)
O(7)	Eu(1)	N(2)	146.9(2)	O(8)	Eu(2)	N(4)	78.4(2)
O(10)	Eu(1)	O(13)	132.7(3)	O(11)	Eu(2)	O(16)	139.5(2)
O(10)	Eu(1)	O(14)	80.7(3)	O(11)	Eu(2)	O(17)	91.4(2)
O(10)	Eu(1)	N(1)	140.4(2)	O(11)	Eu(2)	N(3)	135.5(2)
O(10)	Eu(1)	N(2)	83.7(2)	O(11)	Eu(2)	N(4)	78.2(2)
O(13)	Eu(1)	O(14)	53.7(2)	O(16)	Eu(2)	O(17)	53.2(2)
O(13)	Eu(1)	N(1)	72.0(3)	O(16)	Eu(2)	N(3)	71.9(2)
O(13)	Eu(1)	N(2)	93.3(2)	O(16)	Eu(2)	N(4)	103.2(2)
O(14)	Eu(1)	N(1)	105.2(2)	O(17)	Eu(2)	N(3)	92.0(2)
O(14)	Eu(1)	N(2)	73.4(2)	O(17)	Eu(2)	N(4)	70.6(2)
N(1)	Eu(1)	N(2)	61.8(2)	N(3)	Eu(2)	N(4)	61.4(2)

Eu(1)–N distance (2.625 Å) is larger than the average Eu(2)–N distance (2.610 Å). Compared with the crystallographic data of Eu(*p*-MOBA)<sub>3</sub>:2,2'-bipy [2], the title complex crystallizes in *Pc* space group, *Z* = 2, the latter has *C2/c* space group, *Z* = 4. The average distance of Eu–O bond for the former (2.385 Å) is shorter than that for the latter (2.403 Å), similarly, the average Eu–N distance for the former is shorter than that for the latter although coordination number is the same for the two complexes. It is obvious that the structural difference arises from different positions of the methoxyl group in the benzene ring. The calculated results of the least-squares plane show that all the benzene rings involved in the dimer are planar with the maximum deviation of 0.02(1) Å. The mean deviation of the sets of carbon atoms for the benzene rings from their least-squares plane is 0.009 Å. The dihedral angle between the C34–C39 benzene ring and the C42–C47 benzene ring is 1.05°, which means that these two benzene rings are

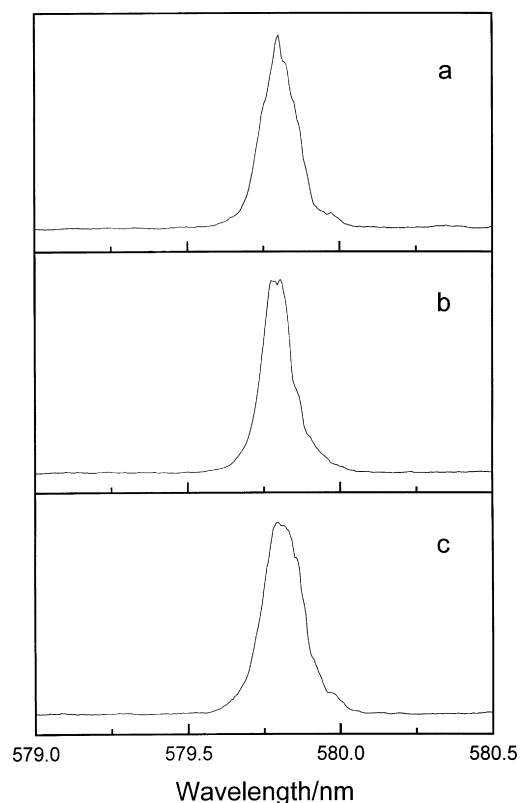


Fig. 3. Excitation spectra of Eu(*m*-MOBA)<sub>3</sub>:2,2'-bipy: (a)  $\lambda_{\text{anal}} = 613.08$  nm; (b)  $\lambda_{\text{anal}} = 616.45$  nm; (c)  $\lambda_{\text{anal}} = 620.39$  nm, 77 K.

parallel. The dihedral angle between each benzene ring attached to the carboxylato-*o,o'* bridge group and the benzene ring containing the chelated carboxylato group can be considered as the same. For instance, the dihedral angle between C2–C7 plane and C32–C37 plane is 31.45° while the angle between C2–C7 plane and C42–C47 plane is 31.67°. The dihedral angle between C26–C31 plane and C34–C39 plane is 40.55°, and the angle between C26–C31 plane and C42–C47 plane is 40.76°. The regular packing for the benzene rings was found in the complex. This may be due to packing effect of aromatic ring, as has been found in the Cu(II) complexes with aromatic amino acids [10]. Furthermore, the bond angle (61.8(2)°) of N(1)–Eu(1)–N(2) of 2,2'-bipy coordinated with Eu(1) is comparable to that (61.4(2)°) of N(3)–Eu(2)–N(4) of 2,2'-bipy coordinated with Eu(2). The bond angle (53.7(2)°) of

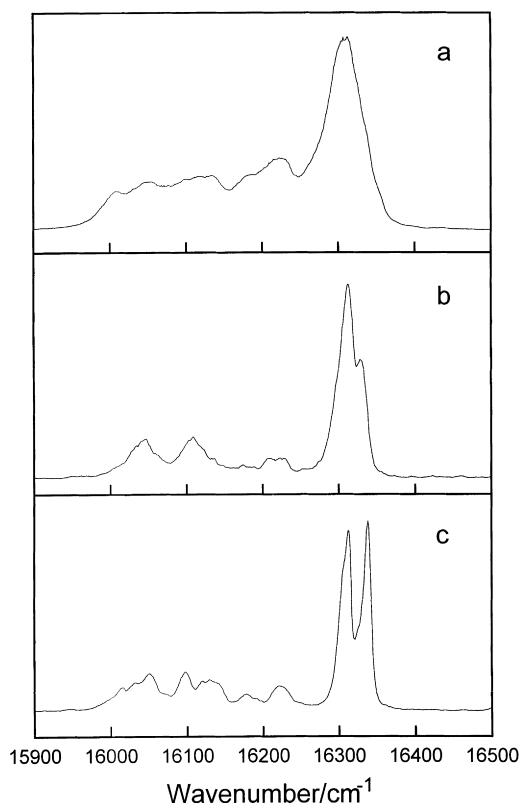


Fig. 4. Luminescence spectra of  $\text{Eu}(m\text{-MOBA})_3 \cdot 2,2'\text{-bipy}$ : (a)  $\lambda_{\text{exc}} = 337.1 \text{ nm}$ ; (b)  $\lambda_{\text{exc}} = 579.90 \text{ nm}$ ; (c)  $\lambda_{\text{exc}} = 579.75 \text{ nm}$ , 77 K.

O(13)–Eu(1)–O(14), composed of Eu(1) and the oxygen atoms of the bidentate chelated carboxylato group is very similar to that ( $53.2(2)^\circ$ ) of O(16)–Eu(2)–O(17) composed of Eu(2) and oxygen atoms of another chelated carboxylato group. The O–C–O angles for the four carboxylato-*o,o'*-bridged groups lie between  $122.4$  and  $126.5^\circ$ .

The time-resolved photoluminescence spectra of  $\text{Eu}(m\text{-MOBA})_3 \cdot 2,2'\text{-bipy}$  obtained using  $337.1 \text{ nm}$  excitation at 77 K is shown in Fig. 2. Fig. 2 shows that intense emission lines of  ${}^5\text{D}_1 \rightarrow {}^7\text{F}_J$  ( $J = 1-3$ ) transitions were observed when delay time was  $2 \mu\text{s}$ , but  ${}^5\text{D}_1 \rightarrow {}^7\text{F}_J$  emission bands disappear after  $20 \mu\text{s}$ . However, emission band intensity of  ${}^5\text{D}_0 \rightarrow {}^7\text{F}_J$  transition increases. This reveals that the lowest triplet state of the ligands is higher than the emission level  ${}^5\text{D}_1$  of the  $\text{Eu}^{3+}$  ion and energy mostly transfers from the triple state of the ligands

*m*-MOBA and 2,2'-bipy to  ${}^5\text{D}_1$  level of the  $\text{Eu}^{3+}$  ion followed by  ${}^5\text{D}_0$  emission level although it is not exclusive that the energy directly transfers from the triplet of the ligands to the lowest emission level  ${}^5\text{D}_0$  of the  $\text{Eu}^{3+}$  ion, and then  ${}^5\text{D}_0 \rightarrow {}^7\text{F}_J$  transition occurs. This also indicates that the  ${}^5\text{D}_1$  state of  $\text{Eu}^{3+}$  is deactivated within  $20 \mu\text{s}$  and the lifetime of the  ${}^5\text{D}_1$  state is much shorter than that of the  ${}^5\text{D}_0$  state of  $\text{Eu}^{3+}$  in the complex.

The  ${}^7\text{F}_0 \rightarrow {}^5\text{D}_0$  transition spectra measured at 77 K upon monitoring the  ${}^5\text{D}_0 \rightarrow {}^7\text{F}_2$  transition are shown in Fig. 3 displaying one band with shoulder. This arises from the fact that free 2,2'-bipyridine is in *trans*-form, but it is in *cis*-form when coordinated with the metal ion. However, coordinated 2,2'-bipyridine may be somewhat different in conformation in the complex. This may be a main reason for the  $\text{Eu}^{3+}$  ions to be surrounded by different chemical environments. Selective excitation on the components of the O–O transition yields emission spectra are shown in Fig. 4b and c. Generally, because of the shielding nature by the outer filled orbitals, perturbation by surrounding neighbours is negligible and characteristic 4f–4f transition sharp line spectra result. However, the emission band (Fig. 4a) obtained upon  $337.1 \text{ nm}$  excitation is an unresolved spectrum which is rarely found in  ${}^5\text{D}_0 \rightarrow {}^7\text{F}_2$  emission spectra of  $\text{Eu}^{3+}$  in complexes. The emission band (Fig. 4a) obtained with non-selective excitation and the emission band (Fig. 4c) recorded using selective excitation which has components more than  $2J + 1$  confirm  $\text{Eu}^{3+}$  ions with slightly different chemical environments in the solid complex. From the curve b in Fig. 4, it can be seen that the emission band composed of lines at  $16329$ ,  $16311$ ,  $16218$ ,  $16108$  and  $16046 \text{ cm}^{-1}$  obtained with lower excitation energy ( $579.90 \text{ nm}$ ) are involved in the emission band (curve c in Fig. 4) obtained with higher excitation energy ( $579.75 \text{ nm}$ ), which obviously illustrates that rapid energy transfer from higher  ${}^5\text{D}_0$  level to lower one occurs when the  $\text{Eu}^{3+}$  ion in the complex is excited with higher excitation energy ( $579.75 \text{ nm}$ ). The average lifetime of the  ${}^5\text{D}_0$  level of  $\text{Eu}^{3+}$  in the complex obtained from the delayed curve is  $1.000 \pm 0.01 \text{ ms}$ .

Supplementary Data relating to this article are deposited with the B.L.L.D. as Supplementary Publication No. SUP26629.

## Acknowledgements

This work is supported by the Natural Science Foundation of Beijing (no. 2982009), National Natural Science Foundation of China (no. 29671003) and the key project of Fundamental Research of Science and Technology, Ministry of China.

## References

- [1] X.M. Zheng, L.P. Jin, M.Z. Wang, J.H. Zhang, S.Z. Lu, Chem. J. Chin. Univ. 15 (1995) 1007 (in Chinese).
- [2] R.F. Wang, L.P. Jin, M.Z. Wang, S.H. Huang, X.T. Chen, Acta Chim. Sin. 53 (1995) 39.
- [3] L.P. Jin, S.X. Lu, S.Z. Lu, Polyhedron 15 (1996) 4069.
- [4] Y. Zhang, L.P. Jin, S.Z. Lu, J. Inorg. Chem. 13 (1997) 280 in Chinese.
- [5] R.F. Wang, L.P. Jin, L.S. Li, S.Z. Lu, J.H. Zhang, J. Coord. Chem. 47 (1999) 279.
- [6] L.P. Jin, R.F. Wang, L.S. Li, S.Z. Lu, S.H. Huang, Polyhedron 18 (1999) 487.
- [7] X. Li, X.J. Zheng, L.P. Jin, S.Z. Lu, W.P. Qin, J. Mol. Struct. (1999) in press.
- [8] N. Walke, D. Stuart, Acta Cryst. A 39 (1983) 158.
- [9] Crystal Structure Analysis Package, Molecular Structure Corporation, USA, 1985 and 1992.
- [10] O. Yamauchi, A. Odani, H. Masuda, K. Toriumi, K. Saito, Inorg. Chem. 28 (1989) 4068.